Proceedings of the 14th IASTED International Conference
Robotics and Applications (RA 2009)
November 2 - 4, 2009 Cambridge, MA, USA

GROUND PLANE DETECTION FOR AUTONOMOUS ROBOTS IN COMPLEX ENVIRONMENTS INCLINED WITH FLEXED FAR-FIELD TERRAINS

Isaac O. Osunmakinde *MIEEE* and Thulani Ndhlovu

Mobile Intelligent Autonomous Systems, Modelling and Digital Sciences Department, Council for Scientific and Industrial Research (CSIR), P O Box 395 Pretoria 0001, South Africa
{iosunmakinde, TNdhlovu}@csir.co.za

ABSTRACT
Ground plane detection is often used as one of the important safety key operations to address some of the issues associated with autonomous navigation in complex environments. Despite the strides on related detection methods developed for such navigation, detection of ground planes inclined with flexed far-fields to alleviate robot short-sightedness, with a guarantee on tarred and coarse terrains have received little attention. Finding a solution to these uncertainty problems is a challenge. In this paper, collective intelligence of the Emergent Situation Awareness (ESA) technology is proposed as a supportive strategy for autonomous robotic navigation. The ability to reveal uncertainties over time on flexed far-field is a ground plane detection strategy embedded in the complex environments. Experimental evaluations of the ESA by benchmarking the results of publicly available roads promise that collective intelligence will one day put an end to most autonomous ground plane detection problems. Such detection on flexed far fields tremendously contributes to good navigational strategies for robotic vehicles being cautious of road accidents.

KEY WORDS
Robotics, Intelligence, Detection, and Emergent Situation Awareness

1. Introduction

Safe autonomous navigation often formulates one of the significant objectives of robotic technology [1]. Researchers and practitioners have stressed that autonomous robotic navigation in complex environments as shown in Figure 1 is an ongoing key challenge [1] [2]. In practice, it is convenient to say that complex environments are relatively defined based on the percentages of mingled features such as collection of colour pixels for ground planes, bushes, and other objects perceived from the left, centre and right sides of the environments. To worsen the situation further, a flexed (or bent) far-field is one of the major roots of fatal accidents for most vehicles and this requires adequate attention.

The complexity of the flexed terrains affects safe navigation and robotic research deliveries, and may hinder the growing usage of robotic vehicles in industries to save lives. Robots for instance, are required to save lives from mining accidents such as 4000 coal miners who died in China in 2006 [3] and 3000 people who were trapped underground in South Africa in 2007 [4]. From our practical knowledge, improving the performance of ground plane detection is obviously a sound basis for optimizing autonomous robotic vehicle navigation.

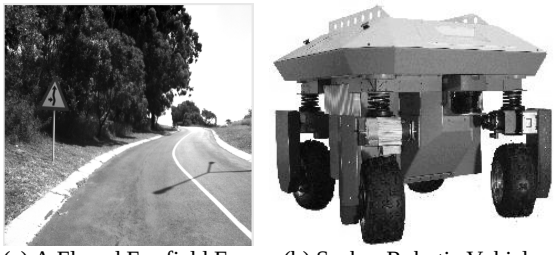

(a) A Flexed Far-field Frame (b) Seekur Robotic Vehicle.

Figure 1: A sampled flexed outdoor road frame and a CSIR four-wheel platform synchronous drive robot, with three pairs of stereo vision cameras.

Researchers [2] have presented related detection methods such as ensemble selection for road image (or frame) segmentations. They develop an individual model for each image segmentation, but the knowledge of their individual models is limited to the features extracted from each frame. There are some significant features which may not be captured from a single image to acquire enough knowledge required to predict far-field grounds. Alternatively, we opined that this can be improved as we use collective intelligence of temporal probabilistic models of the ESA to detect ground planes on flexed far-field terrains. We shall first present the rudimentary details of our detection strategy before its application in robotic vehicles.

Situation Awareness (SA) is to a notable extent becoming popular among decision makers. SA has gained its popularity in, for example, the areas of air traffic control, emergency responders and surgical teams [5]. Instances of application areas where taking correct rapid-response decisions is needed are disaster management,

business intelligence, robotics, even sport (e.g. robotic soccer) where players have to make instant decisions in a constantly changing environment. Most notably, there is an ongoing demand for SA technologies and their variants in environmental water management problems, in areas presenting human health risks, and in robotic agents [6] [7]. Each of these problem areas is too complex to understand due to the uncertainties embedded therein, but compact representation of Bayesian Network (BN) models are effective in handling complexities.

Bayesian Networks (BNs) are probabilistic models which are gaining popularity in decision-making, and are potentially used as robotic module deciding on which field classes are ground planes. The major shortcomings of their current implementations include the inaccurate complex modelling despite expert intervention, and the absence of complete temporal pattern modelling capabilities. The available DBNs (Dynamic Bayesian Networks) with temporal modelling such as; Factorial HMM (Hidden Markov Models), Coupled HMM, Input-Output HMM, and PDBN (partial Dynamic Bayesian Network) [8] [9] have contributed to modelling up to the baseline, but they are explicitly represented by skilled users, therefore are limited in their expressive power. System Engineers such as robotic researchers and non-expert practitioners struggle to interpret and integrate the DBN models to carry out a directed goal. This can make robots to not become well acquainted with the situations of ground planes currently occurring in their various domains. Finding a solution to this issue is a challenge, and the difference between poor and good autonomous navigation lies in their situational understanding of flexed far fields.

In this paper, we achieve emergent situational awareness by evolving actual local dynamics from global emergent behaviour. The global behaviour is the temporal probabilistic model that captures uncertainties of possible ground situations embedded in a number of complex road images. The local dynamics are the smallest pieces of information needed by robots for easily making correct ground plane detection on a frame. This paper aims to empower robotic autonomy using the ESA technology to make the best possible ground detection from any recognized flexed far-field over time. The ESA technology; evolves temporal probabilistic models directly from complex environments captured as MTS (Multivariate Time Series) in the absence of domain experts, views knowledge as situational patterns over time, and provides a suitable platform guide for robots on ground detection processes. The major contributions in this paper are as follows:

- The applications of the collective intelligence of the ESA technology to improve autonomous robot navigation through ground plane detection over flexed, tarred, and coarse far-fields.
- The evaluation of the ESA models by benchmarking publicly available roads and popular image detection methods.

The rest of this paper is arranged as follows: in section 2, we present the theoretical background of the ESA as a class of DBN or temporal probabilistic models. Section 3 presents the proposed technology, which includes the system model and algorithm of the ESA. Section 4 critically presents three experimental applications and evaluations of the ESA on autonomous robotic navigation through ground plane detection. We conclude the paper in section 5.

2. Theoretical Background of the ESA

2.1 Dynamic Bayesian Networks (DBNs)

The simplest form of DBN is shown in Figure 2.

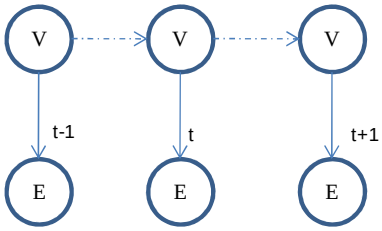

Figure 2: The simplest DBN is Hidden Markov Model with *V* as state variables and *E* as evidence variables repeated in three time steps.

DBNs are temporal probabilistic models which are often referred to as an extension of the Bayesian network (BN) models in artificial intelligence [8]. A Bayesian belief network is formally defined as a directed acyclic graph (DAG) represented as G = {V(G), A(G)}, where V(G) = $\{V_1,\ldots,V_n\}$, vertices (or variables) of the graph G and $A(G) \subseteq V(G) \times V(G)$, is the set of arcs of G. The network requires discrete random values such that if there exists random variables $V_1, \ldots, V_n$ with each having a set of some values $v_1, \ldots, v_n$ then, their joint probability density distribution is defined in equation (1);

$$pr(V_1,...,V_n) = \prod_{i=0}^{n} pr(V_i \mid \pi(V_i)) \quad (1)$$

where $\pi(V_i)$ represents a set of probabilistic parent(s) of child V_i [10]. A parent variable otherwise referred to as *cause* has a dependency with a child variable known as *effect*. This is similar to variables *V* and *E* in a time step of Figure 2. Every variable *V* with a combination of parent(s) values on the graph G captures probabilistic knowledge (distribution) as a conditional probability table (CPT). A variable without a parent encodes a marginal probability. If the environment is small, a BN can be modelled by eliciting the probabilistic knowledge from domain experts. For more complex domains, such as flexed roads, the most suitable Bayesian networks are learned from the environments captured as datasets. Figure 3 illustrates the stages required to learn a BN as a frame model within a time step.

As illustrated in Figure 3, learning such model dynamically from MTS can be decomposed as follows into sub-problems of; (i) data discretization as a pre-processing step, (ii) learning the network structures over time, (iii) learning the associated CPTs (conditional probability tables) over time, and (iv) model visualization. Data discretization classifies numerical data into their corresponding interval values relative to the patterns in the data attributes. Intelligent system researchers such as [11] [12] have presented many algorithms to learn Bayesian networks from datasets. Its characteristics of capturing dependency variables make it suitable for handling complex problems [7].

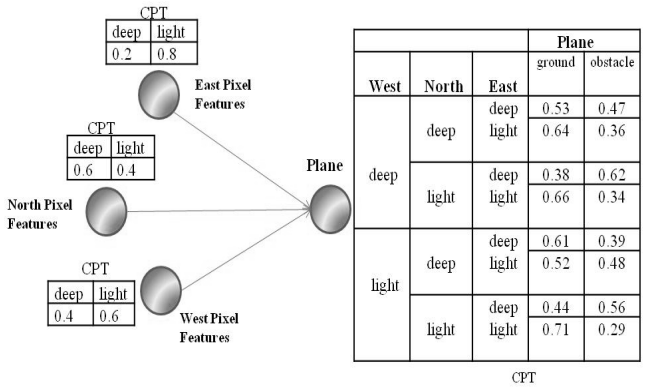

			Plane	
West	North	East	ground	obstacle
deep	deep	deep	0.53	0.47
		light	0.64	0.36
	light	deep	0.38	0.62
		light	0.66	0.34
light	deep	deep	0.61	0.39
		light	0.52	0.48
	light	deep	0.44	0.56
		light	0.71	0.29

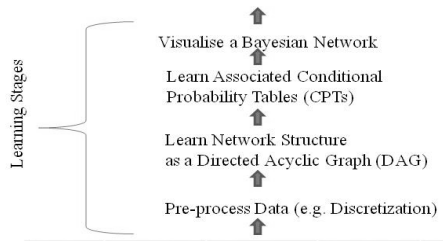

Road Frames	West Pixel Features	North Pixel Features	East Pixel Features	Plane
1	deep	light	deep	obstacle
1	deep	deep	deep	ground
2	light	light	deep	ground
2	light	deep	light	obstacle
2	deep	light	light	obstacle
3	light	light	light	ground
.	.	.	.	.
.	.	.	.	.
n	.	.	.	.

Figure 3: Learning Stages of a BN in a time step.

However, the inability of the BNs to capture time as temporal dependencies facilitated the developments of various ways of modelling the dynamic Bayesian networks presented at the introduction. The variables and the CPTs of the BNs are similar to the states and the probabilities used in the temporal dependencies of the DBNs. According to [7], a DBN is suitable for modelling the environment that emerges (changes) over time and has the capability to predict the future behaviour of the environment. In this research, we want to predict the most likely ground planes on a flexed far-field that a robot must traverse, which is not known based on the current collective closer situations on the frames the robot understands. Most DBNs observe the first-order of Markov model which states that, future event V_{t+1} is independent of the past given the present V_t [7]. It is represented as a transition probability $Pr(V_{t+1} \mid V_t)$. The states of events in a DBN have complex interaction due to the time dependency and may impact on the observed variables of the DBN at any time step.

Let V_i^t represent DBN variables of the ESA at time *t*; we derive the following equation (2) from equation (1), over all the non-negative time steps $t \in T$, where T = {total time steps over the target areas} e.g. road frames, and t = {the time step within the volume of an area} e.g. an image frame.

$$pr(V_1^t, V_2^t ..., V_n^t) = \prod_{i=0}^{n} pr(V_i^t \mid \pi(V_i^t)), \ \forall \ t \in T \qquad (2)$$

The system of equation (2) forms temporal dependency relations between the time slices of model frames as shown in equation (3), which generates a matrix of collective or transition knowledge embedded in the environments captured as MTS.

$$pr(V_1^1, V_2^1 ..., V_n^1) \overset{\Delta}{\equiv} pr(V_1^2, V_2^2 ..., V_n^2) \overset{\Delta}{\equiv} pr(V_1^t, V_2^t ..., V_n^t) \qquad (3)$$

$\overset{\Delta}{\equiv}$ implies that equivalence is *not* true generally.

From equation (3), the relationships embedded among variables *V* at time step 1 may or may not be equivalent to the variables' relationships at time step 2, and for subsequent time steps t. This is as a result of the changes in environmental patterns, which affect the relationships of the model variables over time. Unlike most DBNs in literature, equation (3) is a DBN that varies both its probabilistic distributions and its temporal DAGs by learning directly from MTS, which captures collection of road colour pixels. The relationships here are of greater value to situation awareness because hidden ground planes are revealed over time.

2.2 Situation Awareness

Situation Awareness (SA) refers to, "…the perception of the elements in the environment within a volume of time and space, the comprehension of their meaning, and the projection of their status in the near future [5]." The most established SA theory is described in a popular model of Endsley [5] which describes the current situation model as a mental model at three hierarchical levels. They are levels 1, 2, and 3 of SA corresponding to *perception*, *comprehension* and *projection* respectively. The three components are; the perception of elements in the environment within a volume of time and space, the comprehension of their meaning, and the projection of their status in the near future.

SA therefore enables a robot to detect the presence of ground planes in its domain of interest in order for it to figure out what to do next. Thus, the temporality link between the theory of SA and the theory of DBNs motivated the development of the ESA and its applications in [13].

3. The Proposed Technology for Robotics

3.1 The System Model for the ESA

The system model comprises three essential components which are; learning algorithms, probabilistic distributions, and the trend analysis. The first two components collectively achieve levels 1 and 2 above by discovering the system knowledge of road frames, which are integrated into the third component called the interface (or projection) knowledge. The module in the robot uses this knowledge as a platform to detect or understand the flexed ground planes ahead.

The Learning Algorithms dynamically evolve temporal models from the collection of pixels embedded in the multivariate time series (MTS). The MTS is observed over the collection of closer pixels extracted from some frames and serves as input for the learning model. The algorithms emerge interlink temporal models from *frames 0* to *n*. The existing learning algorithms such as genetic algorithms (GA) [11] [12], which are used for learning BNs from datasets, fit into the ESA, if upgraded to learn over time. The optimized GA in [12] is upgraded to evolve over time and is used as a proof of concept in this system model. The algorithm uses information-theoretic measures (e.g. Minimum Description Length) and mathematical components (e.g. PowerSet in set theory) as genetic operators and as a means of balancing between efficiency and decomposability. The GA is used due to its efficiency as it performs very well when used to emerge models from the environments of numerical, nominal, and mixed datasets.

The other functionality of the probabilistic distribution of the system model is a Bayesian inference of the Variable elimination algorithm [7], which is used to reason and detect over time. This reasoning algorithm is based on Bayes' theorem [10], expressed as posterior probability in equation (4) for some random variables V_s and V_e. The V_s implies state variable of the model while V_e implies evidence variable.

$$\Pr(V_S \mid V_e) = \frac{\Pr(V_e \mid V_S) * \Pr(V_S)}{\Pr(V_e)} \qquad (4)$$

The component of trend analysis is an interface that constructs a transition matrix of knowledge on ground planes over time. The nature of knowledge on the patterns generated determines the likely navigation or action taken by the robot on any ground situation *n* to arrive at (or avoid) the next ground situation *n+1*. In applying this technology, especially by robotic researchers or non-expert practitioners, we formally present the ESA algorithm as shown in Figure 4.

3.2 The ESA Algorithm

An MTS serves as the required schema to Figure 4 but the additional capability of the ESA algorithm in Figure 4 serves to generate MTS from domain datasets without changing their originalities. Its development is based on the theories, algorithms, models, and mathematical equations that are used as subroutines as presented in the previous sections.

INPUT (D_s : Dataset Schema)

---

1. While D_s = MTS,
   - [i] If D_{sj} = *Numeric*, for j = 0, 1, 2. . . m.
     - Call Scalable_Discretizer (D_{sj}).
   - [ii] Perform ordering on D_s using t key.
   - [iii] Set t, the frame count, to *0*.
   - [iv] Let $d_t \in D_s$, $\forall$ t = 0, 1, 2, . . ., n.
   - [v] For each $t <= n$,
     - Select frame d_t for emergence.
     - Call Bayesian_Learner (d_t).
     - Store the emerged temporal BN in matrix *B*.
     - Increment t by 1.
   - [vi] For Situational Trends, Call Probabilistic Distributions, $\forall$ $b_t \in B$.
   - [vii] Return the dynamic BNs in *B* as the frames' situations, then exit.
2. While D_s <> MTS,
   - [viii] If D_{sj} = *Date*,
     - Select t.
     - Generate MTS from D_s using t.
   - [ix] Repeat step 1.

Figure 4: Emergent Situation Awareness (ESA) Algorithm

In Figure 4, the D_{sj} is a column of the schema, d_t is a frame dataset and b_t is a temporal Bayesian Network emerged at time t. As shown in step 1[*i*], discretization classifies numerical datasets into their corresponding interval values relative to the patterns in the data attributes. Due to the predominance of computational intensity during data-preprocessing, the ESA introduces scalability into the discretization processes. In this scheme, space is shared and every used memory is cleared for the next processes. In step 1[*v*], the Bayesian learners are any of the algorithms that were recently mentioned [11] [12], whose functionalities are to carry out intra-slice learning over time. They emerge temporal optimal BN at each time step. Likewise, the Bayesian inference generates several situational trends as a

transition matrix of knowledge, which is consequently used to reveal ground planes over the flexed far-fields.

Revealing hidden ground planes is made simpler with the ESA, as robots can now be well acquainted with their current domains before projecting into the complex far-field. Since the ESA is domain-independent, it not only accommodates highly skilled users, but also allows non-expert robotic practitioners to benefit from the temporal probabilistic modelling.

4. Experimental Evaluations on Ground Plane Detection for Robotic Vehicles

One of the objectives of this paper is to bring the theory of the ESA technology to practice with an emphasis on robotic applications and practical work on ground plane detection. This consequently alleviates the robot's short-sightedness as it detects ground planes over complex flexed far-fields. It is an optimization strategy for autonomous robotic vehicle navigation.

To justify the universality of the ESA and to assure that our modelling design is reproducible, real life and publicly available road images are used to benchmark our theories and implementations. Three experiments were conducted on five flexed terrains (tarred and coarse) including (1) CSIR real life road frames captured locally, (2) public road images with ensemble selection [2], and (3) public road frames collected by a robotic vehicle [14]. The performance accuracies of the ESA detection on each of these frames are also computed using the cross validation technique and summarised as confusion matrix described by [15]. With cross-validation, a fraction of the known data is set aside by using it to test the detection of a hypothesis induced from the remaining data [7]. With five known ground planes and five known obstacles on Figures 5 to 9, we randomly set aside ten frame points from the middle to the far end on each of the original frames as expected results. They are compared with the ESA detection results, which are visualized as confusion matrices. It is a matrix of tabular structure that contains the number of expected and detected ground planes, and obstacles using the ESA model. The performance accuracy of the detection is computed as α from the matrix as expressed in equation (5). In Figure 5c for example, α = ((5+5)/(5+0+0+5)) * 100% = 100%.

$$\alpha = \frac{\sum(Left\_diagonal\_entries)}{\sum(All\_entries)} \times 100\% \qquad (5)$$

4.1 Experiment 1: Illustrating Ground Plane Detection with CSIR Tarred Roads

Streams of flexed frames are perceived locally from CSIR tarred roads, such as the examples shown in Figures 1a and 5a. The objective here is to detect ground planes especially towards the bent far-fields. A MTS was captured from these complex frames, where collections of pixel colours are extracted from each frame point P_i. This is iterated over 80 by 100 grid points with the horizon being ignored (or cut-off). The frames run through an image processing tool in MATLAB, where analysis per pixel with a 9 by 9 support window is carried out. This analysis operates on a defined colour band in the RGB colour space. The instances of the image pixels collections are trained and labelled as ground and obstacles. The closest collections of pixels to the robot's view on a number of frames are used as training data while the far-field pixels are unknown to the model emerged by the ESA for detection purposes within a volume of time space.

$$pr(\textbf{Plane}^t ? \mid P_1^t = 20\%, P_2^t = 74\%, P_3^t = 84\%, \ldots, P_{n-2}^t = 84\%, P_{n-1}^t = 87\%, P_n^t = 45\%) \qquad (6)$$

Using the Bayes' theorem in equation (4), equation (6)

$$\Rightarrow \frac{\Pr(P_1^t = 20\%,\ldots, P_n^t = 45\% \mid Plane^t) \times \Pr(Plane^t)}{\Pr(P_1^t = 20\%,\ldots, P_n^t = 45\%)}$$

This is a Bayesian inference problem with more information in [7].

(a) Flexed Tarred Road

(b) ESA Detection

Expected	Detected	
	Ground Plane (GP)	Obstacles (Ob)
Ground Planes (5)	**5**	0
Obstacles (5)	0	**5**

(c) Confusion Matrix with detection accuracy 100%

Figure 5: (a) CSIR original road image, (b) ignoring the horizon, detected ground plane depicted as green (or light) colour and obstacles depicted as red (or dark) on a flexed tarred field, and (c) the ESA accuracy visualized as confusion matrix.

Having obtained the model of the target environments, the robot acquires collective knowledge and acts on these frames in real time (during autonomous navigation) to detect ground planes on the flexed far-field. An effective

stereo camera mounted on the Seekur robot perceives new environmental frame features from a long range, whose colour pixels collections are used to query the tarred road model within a space of time and enable the robot to detect the ground planes on CSIR roads. A probabilistic query example is illustrated in equation (6) and its detected results are shown in Figure 5 with the accuracy captured as confusion matrix.

On the query situation in equation (6), the robot wants to know within a space of time, the *most* probable planes of Figure 5a for example, when the features situation (e.g. P_1 = the first frame point colour with grey saturation 20%, P_n = the last frame point colour with grey saturation 45%, etc.) are perceived over a distance. The detection is a continuous process as the robot perceives new features as evidences over time. One can see in Figure 5 that the ESA adequately detects the complex flexed far terrain to avoid accidents. For the confusion matrix results, the number of correct detections that image instances are ground plane and obstacles are five each. Therefore, performance is ((5+5)/(5+0+0+5)) * 100% = 100% detection accuracy. Here, our results guarantee ground plane detection on tarred flexed far-fields.

4.2 Experiment 2: Benchmarking the ESA Technology with Ensemble Selection Outputs on Coarse Roads

A good and related work is from Procopio et al. [2] who used publicly available coarse road images with ensemble selection as shown in Figures 6 and 7. They suggested comparisons of other techniques like ours to their ensemble selection for possible performance benefits. They sampled near-field labels to create training sets, extracted features for learning and storing the individual terrain model as a model library while they used SVM as a base learner and ensemble selection for classification. As shown in Figures 6b and 7b, they indicated very dark colour with uncertainty, obstacles with red (or dark), and ground planes with green (or light) colours. One of their major challenges is computational intensity which we do not experience as we collect the pixels into numerous grid points. As presented at the introduction, the knowledge of their individual model is limited to the features extracted only from each frame.

For the purpose of aligned comparison, we improve on this as the ESA model collects knowledge from the closer features on a number of frames before detecting the new far-field pixels on the frames as shown in Figures 6c and 7c. A similar pixel modelling procedure of experiment one is repeated here except that we define a range of colour bands on a brownish scale and as RGB colour space. The results depicted by the confusion matrix are a summary of the detection of the ESA using the cross validation technique in terms of expected and detected planes. Examples of test features situations are $s_1 = \{ P_1^{\,t} = 20\%, P_2^{\,t} = 55\%, P_3^{\,t} = 54\%, ..., P_n^{\,t} = 36\% \}$ from Figure 6a and $s_2 = \{ P_1^{\,t} = 20\%, P_2^{\,t} = 50\%, P_3^{\,t} = 59\%, ..., P_n^{\,t} = 37\% \}$ from Figure 7a. The test situations, s_i, in equations (7) and (8) are used similarly for detection like the probabilistic query in equation (6).

$$pr(\textbf{Plane}^t ? \mid P_1^{\,t} = 20\%, P_2^{\,t} = 55\%, P_3^{\,t} = 54\%, ..., P_n^{\,t} = 36\%) \quad (7)$$

$$pr(\textbf{Plane}^t ? \mid P_1^{\,t} = 20\%, P_2^{\,t} = 50\%, P_3^{\,t} = 59\%, ..., P_n^{\,t} = 37\%) \quad (8)$$

(a) Flexed Coarse Frame

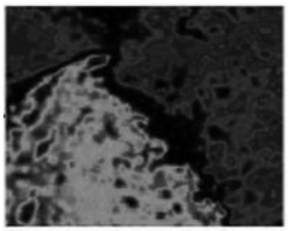

(b) Ensemble Detection

(c) ESA Detection

Expected	Detected	
	GP	Ob
Ground Plane(GP) (5)	**5**	0
Obstacles (Ob) (5)	1	**4**
Accuracy	90%	

(d) Confusion Matrix

Figure 6: (a) First original coarse road image [2], (b) its detection result using ensemble [2], (c) detected ground plane depicted as green (or light) colour and obstacles depicted as red (or dark) on a flexed coarse field, and (d) the ESA accuracy visualized as confusion matrix.

(a)Original Coarse Frame

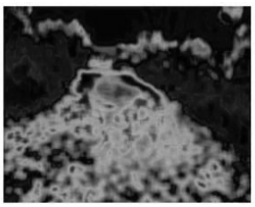

(b) Ensemble Detection

(c) ESA Detection

Expected	Detected	
	GP	Ob
Ground Plane(GP) (5)	**4**	1
Obstacles (Ob) (5)	0	**5**
Accuracy	90%	

(d) Confusion Matrix

Figure 7: (a) Second original coarse road image [2], (b) its detection result using ensemble [2], (c) detected ground plane depicted as green (or light) colour and obstacles depicted as red (or dark) on a coarse field, and (d) the ESA accuracy visualized as confusion matrix

One can see in Figures 6 and 7 that the ESA detects on coarse ground planes similarly to ensemble selection outputs but with more capability in handling the uncertainties over time, especially on the flexed far terrain. On the confusion matrix results, observe the performance detection accuracies of 90% for Figures 6 and 7. Here, our results also guarantee improved ground plane detection on coarse far-fields due to the collective intelligence of the ESA models than Figures 6b and 7b.

4.3 Experiment 3: Benchmarking the ESA Results with Other Coarse Ground Planes

In order to ascertain the performance of the ESA on ground plane detection for robots, we also benchmark it with the results of other relevant public coarse road images collected by robotic vehicle [14], whose examples are shown in Figures 8 and 9. They were provided with labelled colours; the light blue results depict the ground plane, the red (or dark) class depicts grass, the yellow (or lightest) class depicts tall vegetation and the deep blue (or very dark) result corresponds to uncertain portion. Though it is not certain on the method used, their results seem good. They also provided these results for further comparative studies as presented herein. The objective here is focused on ascertaining the performance of the ESA in detecting ground planes on coarse flexed roads.

(a) Flexed Coarse Frame

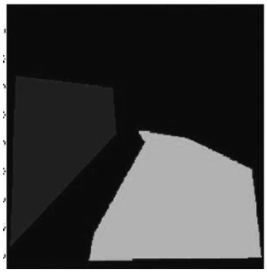

(b) Repository Results

(c) ESA Detection

Expected	Detected	
	GP	Ob
Ground Plane(GP) (5)	**4**	1
Obstacles (Ob) (5)	1	**4**
Accuracy	80%	

(d) Confusion Matrix

Figure 8: (a) Other original coarse road image [14], (b) its provided repository result [14], (c) ignoring the horizon, detected ground plane depicted as green (or light) colour and obstacles depicted as red (or dark) on a flexed coarse field, and (d) the ESA accuracy visualized as confusion matrix.

An MTS was captured from these frames, where collections of pixel colours are extracted from each frame point similarly to experiment one. We also set a range of colour saturation but on brownish colour bands as a subspace of RGB colours. The closest collections of pixels to the robot's view are used as MTS training while the far-field pixels are detected by the ESA within a volume of time space. Examples of test features situations that can be perceived by the robot stereo camera are $s_3 = \{ P_1^{\,t} = 20\%, P_2^{\,t} = 76\%, P_3^{\,t} = 77\%, ..., P_n^{\,t} = 40\% \}$, from Figure 8a and $s_4 = \{ P_1^{\,t} = 25\%, P_2^{\,t} = 65\%, P_3^{\,t} = 63\%, ..., P_n^{\,t} = 43\% \}$ from Figure 9a. The test situations, s_i, are used similarly for detection like the probabilistic queries in equations (7) and (8) of experiment two respectively. The sampled results depicted by the confusion matrix are summarised as expected and detected planes and obstacles.

Once again, one can see in Figures 8 and 9 that the ESA detects the coarse ground planes adequately as the benchmark results but with more capability in handling the uncertainties especially on the flexed far terrain. On the confusion matrix results, observe the performance detection accuracies of 80% and 100% for Figures 8 and 9 respectively. Here, our results once again guarantee improved ground plane detection on coarse flexed far terrain than Figures 8b and 9b.

(a) Flexed Coarse Frame

(b) Repository Results

(c) ESA Detection

Expected	Detected	
	GP	Ob
Ground Plane(GP) (5)	**5**	0
Obstacles (Ob) (5)	0	**5**
Accuracy	100%	

(d) Confusion Matrix

Figure 9: (a) Another original coarse road image [14], (b) its provided repository result [14], (c) detected ground plane depicted as green (or light) colour and obstacles depicted as red (or dark) on a flexed coarse field, and (d) the ESA accuracy visualized as confusion matrix.

5. Conclusion and Future Work

In this paper, we have presented the theory and applications of the collective intelligence of the ESA technology to improve autonomous robot navigation through ground plane detection over flexed, tarred, and coarse far-fields. This study shows that one day the ESA will potentially put an end to all ground plane detection problems of robotic vehicles as it contributes to improve autonomous navigation.

This technology emerges temporal probabilistic models from complex environments captured as multivariate time series (MTS), acts on this model, and detects ground planes for robots. Its critical evaluations measure its overall detection accuracy as 92% from confusion matrices of experiments one to three. The results of Figure 5 guarantee that the ESA detects ground planes accurately on tarred roads. Also, the results of Figures 6 to 9 show that the ESA can detect ground planes on coarse fields similarly to ensemble selection outputs and the repository road image results but with more capability in handling uncertainties, especially on the flexed far-field terrains. The good performance of the ESA on ground plane detection for robotic vehicles is as a result of its collective intelligence paradigm. Though we are not currently experiencing computational intensity, we are working to make our idea robust by carrying out a sensitivity analysis on texture component and ensure scalability of the ESA ground plane detection to handle possible massive MTS for robots.

Acknowledgements

The authors gratefully acknowledge resources and financial supports from the Council for Scientific and Industrial Research.

References

[1] J. Minguez, & L. Montano, Sensor-Based Robot Motion Generation in Unknown, Dynamic and Troublesome Scenarios, *Journal of Robotics and Autonomous Systems*, 52, 2005, 290-311.

[2] M.J. Procopio, J. Mulligan, & G. Grudic, Learning in dynamic environments with Ensemble Selection for autonomous outdoor robot navigation, *IEEE/RSJ International Conference on Intelligent Robots and Systems*, ISBN: 978-1-4244-2057-5, 2008, 620-627.

[3] Australian online newspaper of the year, http://www.theaustralian.news.com.au/story/0,20867,20749177-1702,00.html, 2006.

[4] Miners trapped underground in South Africa, Independent students daily newspaper, University of Illinois, Associated Press, http://www.dailyillini.com/, 2007.

[5] M.R. Endsley, *Theoretical underpinnings of situation awareness: a critical review, Situation Awareness Analysis and measurement* (Mahwah, NJ: Lawrence Erlbaum Associates, 2000).

[6] W.A. Pike, Modelling Drinking Water Quality Violations With Bayesians Networks, *Journal of the American Water Resources Association (JAWRA)*, 40, 2004, 1563 – 1578.

[7] S. Russell, & P. Norvig, *Artificial Intelligence* (A Modern Approach, 2nd Edition, Prentice Hall Series Inc. New Jersey 07458, 2003).

[8] K. Murphy, *Dynamic Bayesian networks representation, inference and learning* (PhD thesis, UC Berkeley, Computer Science Division, 2002).

[9] K.C. Chang, Almost Instant Time Inference for Hybrid Partially Dynamic Bayesian Networks, *IEEE Transactions on Aerospace and Electronics Systems*, 43, 2007.

[10] J. Pearl, *Probabilistic reasoning in intelligent systems, networks of plausible inference*, (Morgan Kaufmann Publishers, 1988).

[11] P. Larranaga, C. Kuijpers, R. Murga, & Y. Yurramendi, Learning Bayesian Network Structures by Searching for the Best Ordering with Genetic Algorithms, *IEEE Transactions on Systems, Man, and Cybernetics*, 1996, 487-493.

[12] I.O. Osunmakinde, & A. Potgieter, Emergence of Optimal Bayesian Networks from Datasets without Backtracking using an Evolutionary Algorithm. *Proceedings of the Third IASTED International Conference on Computational Intelligence*, Banff, Alberta, Canada, ACTA Press, ISBN: 978-0-88986-672-0, 2007, 46 - 51.

[13] J.K. Balikuddembe, I.O. Osunmakinde, & A.E. Potgieter, Software Project Profitability Analysis Using Temporal Probabilistic Reasoning, In *Proceedings of the Advanced Software Engineering and Its Applications - ASEA. IEEE Computer Society, Washington, DC,* ISBN: 978-0-7695-3432-9, 2008, 99-102.

[14] Bayesian Fusion Datasets Repository http://italia.cse.ucsc.edu/~manduchi/FusionDataSets/Road.html

[15] R. Kohavi, & F. Provost, Special Issue on Applications of Machine Learning and the Knowledge Discovery Process. *Journal of Machine Learning, Kluwer Academic Publishers*, 1998, 271-274.